nature chemical biology

ARTICLES

https://doi.org/10.1038/s41589-019-0401-8

Discovery of an antivirulence compound that reverses β-lactam resistance in MRSA

Omar M. El-Halfawy[1,2,3], Tomasz L. Czarny[1,2], Ronald S. Flannagan[4], Jonathan Day[5], José Carlos Bozelli Jr.[1], Robert C. Kuiack[4], Ahmed Salim[5], Philip Eckert[6], Richard M. Epand[1], Martin J. McGavin[4], Michael G. Organ[5,6], David E. Heinrichs[4] and Eric D. Brown[1,2*]

Staphylococcus aureus **is the leading cause of infections worldwide, and methicillin-resistant strains (MRSA) are emerging. New strategies are urgently needed to overcome this threat. Using a cell-based screen of ~45,000 diverse synthetic compounds, we discovered a potent bioactive, MAC-545496, that reverses β-lactam resistance in the community-acquired MRSA USA300 strain. MAC-545496 could also serve as an antivirulence agent alone; it attenuates MRSA virulence in** ***Galleria mellonella*** **larvae. MAC-545496 inhibits biofilm formation and abrogates intracellular survival in macrophages. Mechanistic characterization revealed MAC-545496 to be a nanomolar inhibitor of GraR, a regulator that responds to cell-envelope stress and is an important virulence factor and determinant of antibiotic resistance. The small molecule discovered herein is an inhibitor of GraR function. MAC-545496 has value as a research tool to probe the GraXRS regulatory system and as an antibacterial lead series of a mechanism to combat drug-resistant Staphylococcal infections.**

S. aureus is the leading cause of both hospital and community-associated infections worldwide and a principle cause for morbidity and mortality[1], especially with the emergence and rapid spread of MRSA, which is resistant to all known β-lactam antibiotics[2]. Worse yet, resistance to vancomycin, linezolid and daptomycin have already been reported in clinical MRSA strains, compromising the therapeutic alternatives for life-threatening MRSA infections[3]. The most serious infections such as endocarditis, osteomyelitis, necrotizing pneumonia and sepsis occur when dissemination of the bacteria into the bloodstream occurs[4].

Among the currently approved antimicrobials, the latest discovery of a new drug class occurred more than 30 years ago. To bridge this discovery gap, various strategies have been investigated including the use of antimicrobial adjuvants. These are molecules that inhibit a bacterial resistance mechanism to an existing antibiotic, effectively increasing bacterial susceptibility to that drug and reviving its clinical utility[5]. Another strategy is to target pathogen virulence, but not growth or viability. This approach is gaining interest because the desired antivirulence agents may not impose the strong selective pressures on bacteria that favor evolution of resistance and persistence mechanisms, and, as they do not affect viability, they should not disrupt beneficial flora[6].

Here we aimed to combine these strategies for enhanced therapeutic potential and sought to discover an inhibitor with dual action: attenuating virulence and reversing antibiotic resistance. Our work began with a cell-based, high-throughput screen to identify molecules that target cell-envelope-related virulence factors. We used a screening platform that detects antagonism of a lethal concentration of targocil, a chemical inhibitor of the wall teichoic acid (WTA) flippase TarG[7], against *S. aureus*. WTA are phosphate-rich polymers that make up a large proportion of the cell wall of Gram-positive bacteria and that have important roles in virulence and resistance to β-lactam antibiotics[8]. WTA biosynthesis is encoded by genes that exhibit paradoxical dispensability patterns[9–11]: genes encoding early steps in the pathway (*tarO* and *tarA*) are dispensable, whereas those encoding late steps (such as *tarG*) cannot be deleted, unless flux into the pathway is prevented, for example, by deleting either *tarO* or *tarA* (Supplementary Fig. 1). This unique dispensability pattern provided the basis for a cell-based screening platform for antagonism of the lethal action of late-step inhibitors such as targocil (Supplementary Fig. 1) that successfully captured inhibitors of the early steps of WTA biosynthesis[12] and of cell-wall biogenesis components that feed into the WTA pathway, namely the undecaprenyl diphosphate synthase UppS[13,14]. These inhibitors potentiated the activity of β-lactams[12–14]. Other cell-envelope-related genes are connected to the WTA pathway through synthetic lethal interactions, for example, genes encoding the lipoteichoic acid (LTA) synthase LtaS, the machinery for D-alanylation of both LTAs and WTAs (DltABCD), and members of a regulatory protein complex comprising a signaling system (GraXRS) and an ABC transporter (VraFG)[15]. Consequently, we hypothesized that the targocil-antagonism screen might also detect inhibitors of these cell-envelope-related components, and that such inhibitors should resensitize MRSA to β-lactam antibiotics.

Using this screening platform, we discovered an inhibitor of GraR, MAC-545496. GraR (glycopeptide-resistance-associated protein R, also known as ApsR, antimicrobial-peptide sensor protein R) is a response regulator protein of a multicomponent regulatory system including the sensor kinase GraS, a signal transduction accessory protein GraX that is associated with the ABC transporter VraFG[16]. Among the GraR-regulated genes are *mprF* and *dltABCD*, encoding proteins that add lysine to membrane phospholipids and

[1]Department of Biochemistry and Biomedical Sciences, McMaster University, Hamilton, Ontario, Canada. [2]Michael G. DeGroote Institute of Infectious Disease Research, McMaster University, Hamilton, Ontario, Canada. [3]Microbiology and Immunology Department, Faculty of Pharmacy, Alexandria University, Alexandria, Egypt. [4]Department of Microbiology and Immunology, The University of Western Ontario, London, Ontario, Canada. [5]Department of Chemistry, York University, Toronto, Ontario, Canada. [6]Centre for Catalysis Research and Innovation (CCRI) and Department of Chemistry and Biomolecular Sciences, University of Ottawa, Ottawa, Ontario, Canada. *e-mail: ebrown@mcmaster.ca

D-alanine to cell-wall teichoic acids, respectively, to increase the positive charge of the surface[17,18]. Its regulon responds to insults to the bacterial cell envelope by factors that contribute to host innate immunity such as cationic antimicrobial peptides (CAMPs) and oxidative stress[17,19,20]. GraR and its regulatory system are important for virulence of *S. aureus*; mutants are attenuated in vivo in different animal models of infection[17,19–22], abrogated for intracellular replication and survival[21] and defective for biofilm formation under certain conditions[23].

MAC-545496 shows potency in the nanomolar range, reversing β-lactam resistance in MRSA and synergizing with CAMPs. Alone, it shows remarkable activity in macrophages and attenuates *S. aureus* virulence in a *G. mellonella* larvae infection model. This work provides a proof of principle for antibacterial compounds that have dual antivirulence and antimicrobial adjuvant properties. The work described herein provides a new research tool to probe the GraXRS regulatory system and an antibacterial lead series of a new chemical class and mechanism, expanding the possibilities for the fight against drug-resistant Staphylococcal infections.

Results

High-throughput screening and hit prioritization. We screened a library of ~45,000 diverse synthetic small molecules (sourced from ChemDiv and ChemBridge) at 20 μM for targocil antagonism, that is, growth rescue in the presence of 8× the minimum inhibitory concentration (MIC) of targocil (16 μg ml^{-1}) in duplicate against *S. aureus* Newman (Supplementary Table 1). The screening parameters were carefully designed (inoculum size of between ~2×10^5 and 5×10^5 colony-forming units (CFU) ml^{-1}, endpoint before observation of suppressor mutants) to minimize the detection of spontaneous suppressors of targocil, which has a relatively high frequency of resistance (>10^{-6})[24]. This resulted in a high degree of reproducibility (99.19% replication rate). This screen yielded 544 primary targocil antagonists detected in both replicates (~1.21% hit rate; Fig. 1a and Supplementary Fig. 2a); additionally, 364 molecules showed growth rescue in only one of the replicates, which is likely due to spontaneous suppressors to targocil and not true antagonism (Supplementary Fig. 2a).

Seeking compounds with the ability to synergize with β-lactams, we performed a secondary screen of these active compounds at a concentration of 10 μM for potentiation of the β-lactam cefuroxime at one eigth of the MIC (64 μg ml^{-1}) against *S. aureus* USA300 (performed in duplicate). This strain is a pandemic hypervirulent community-acquired MRSA, which is the most prevalent MRSA strain in North America, and has spread worldwide[25]. This secondary screen revealed nine potent β-lactam synergizers (Fig. 1a and Supplementary Fig. 2b). We performed dose-dependent analyses to rank these actives (Supplementary Fig. 3); MAC-545496 (**1**) and MAC-533252 (**2**) showed the most potent synergism with cefuroxime. Interestingly, both compounds were structural analogs that both have a benzoyl thiourea moiety (Supplementary Fig. 3). Other compounds (MAC-534930 (**3**) and MAC-535051 (**4**)) possessed the central carbonyl thiourea moiety but showed lower activity (Supplementary Fig. 3). MAC-533252, however, showed solubility issues in the test culture medium hindering further characterization and was deprioritized. MAC-545496 was resupplied and its synergy with β-lactams and antagonism with targocil was reconfirmed (Supplementary Fig. 4). Importantly, MAC-545496 reversed the β-lactam resistance of MRSA USA300. Clinical Laboratory Standards Institute (CLSI) guidelines recommend using oxacillin sensitivity to determine methicillin resistance in *S. aureus*[26]. A very low-dose of MAC-545496 (0.06 μg ml^{-1}, which is equivalent to ~150 nM) was sufficient to lower the oxacillin MIC to below the CLSI clinical breakpoint (Fig. 1b); *S. aureus* is deemed to be methicillin sensitive at MIC values less than this breakpoint. MAC-545496 potently synergized with cefuroxime; concentrations as low as 0.03 μg ml^{-1} (~75 nM) lowered the β-lactam MIC from 512 to 8 μg m^{-1} against *S. aureus* USA300 (Supplementary Fig. 4a). MAC-545496 also synergized with cefuroxime and oxacillin against a collection of ten *S. aureus* clinical isolates (Supplementary Table 2). In addition, MAC-545496 potentiated the effect of cefuroxime against representatives of other circulating MRSA strains such as USA100, USA400 and USA500 to different extents, with the exception of CMRSA4, a USA200/EMRSA16 isolate (Supplementary Table 3). In methicillin-sensitive *S. aureus* (MSSA) isolates, we detected modest potentiation by MAC-545496 (two- to fourfold reduction in cefuroxime MIC), as these strains are already sensitive to β-lactams (Supplementary Table 3). Remarkable synergy against *S. aureus* USA300 was observed with all other tested β-lactams: penicillins (methicillin, nafcillin and piperacillin); cephalosporins (cefadroxil, cefaclor, ceftizoxime and ceftazidime); and the carbapenem imipenem (Supplementary Fig. 5). MAC-545496 also synergized with the antimicrobial peptides colistin and polymyxin B (Supplementary Figs. 5 and 1c, respectively). Modest potentiation (two- to fourfold change in MIC) occurred with gentamicin, daptomycin, bacitracin and vancomycin, while no change was observed with tetracycline, chloramphenicol, azithromycin, rifampicin, novobiocin, ciprofloxacin, D-cycloserine and sulfamethoxazole (Supplementary Fig. 5).

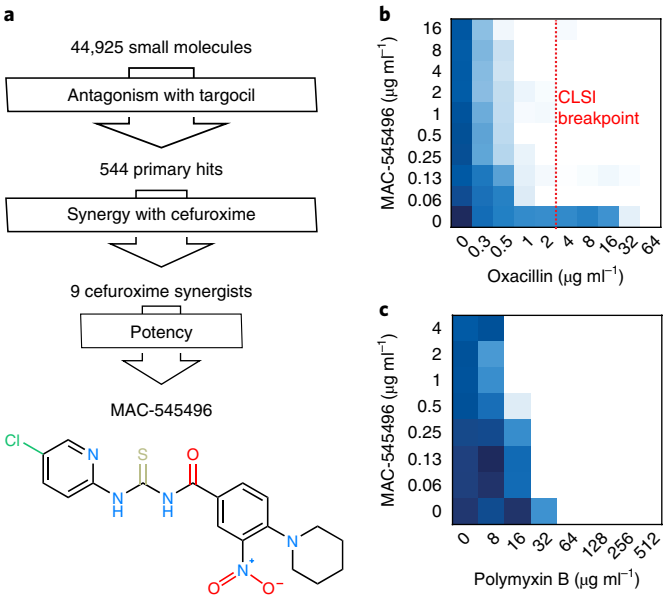

Fig. 1 | High-throughput screening identifies potent bioactives that reverse β-lactam resistance in MRSA. a, The workflow undertaken in this study. **b**, Representative checkerboard assay against *S. aureus* USA300 of MAC-545496 with oxacillin indicating the clinical breakpoint set by the CLSI (FICI ≤ 0.0332). Note that 0.06 μg ml^{-1} MAC-545496 is equivalent to ~150 nM. **c**, Representative checkerboard assay of MAC-545496 with polymyxin B against *S. aureus* USA300 (FICI ≤ 0.2812). These checkerboards were repeated three times independently, yielding similar results.

Mode of action determination. MAC-545496 does not exhibit intrinsic growth inhibitory activity against *S. aureus*; therefore, we reasoned that it targets the product of a non-essential gene. First, we used a chemical–genomic approach to study the mechanism of MAC-545496. This included a screen of the Nebraska transposon mutant library (NTML), a sequence-defined *bursa aurealis* transposon (Tn) mutant library consisting of 1,920 strains, each containing a single mutation covering the non-essential genes of *S. aureus* USA300 (ref. [27]). We hypothesized that a mutant in the gene encoding the target of MAC-545496 would be significantly less resistant

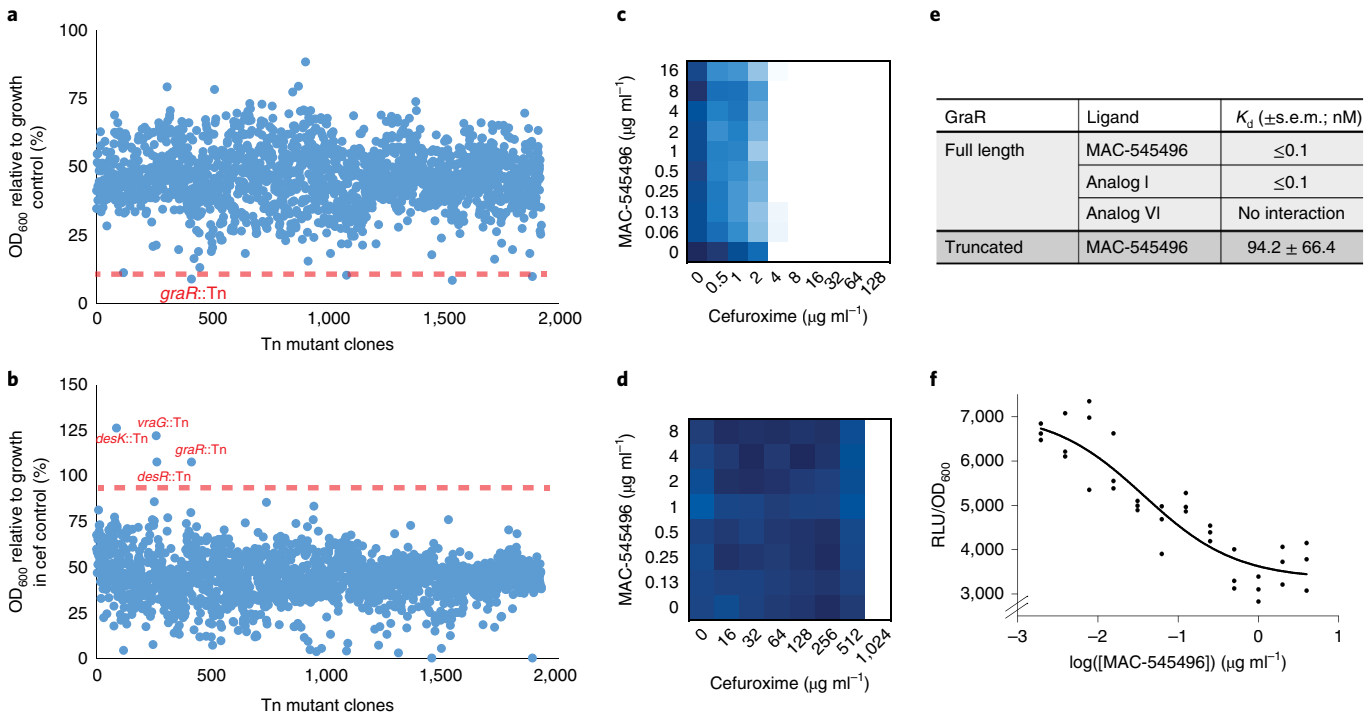

GraR	Ligand	K_d (±s.e.m.; nM)
Full length	MAC-545496	≤0.1
	Analog I	≤0.1
	Analog VI	No interaction
Truncated	MAC-545496	94.2 ± 66.4

Fig. 2 | MAC-545496 targets GraR, a regulator of the cell-envelope stress response. a,**b**, Screening of the NTML covering the non-essential genes in *S. aureus* USA300 in the presence of 16 μg ml^{-1} of cefuroxime alone (**a**; data are shown as a percentage of growth of each clone in the presence of cefuroxime relative to its respective control growing in CAMHB medium) and in combination with 1 μg ml^{-1} of MAC-545496 (**b**; data are shown as a percentage of growth of each clone in the presence of the combination relative to its respective growth in the presence of cefuroxime alone). Data are the mean of two repeats. **c**,**d**, Representative checkerboard assays of MAC-545496 and cefuroxime against the *graR*::Tn mutant (**c**) and spontaneous resistant mutants in which MAC-545496 lacked activity (**d**; G217* GraR, clone 8). FICI ≥ 1 for both checkerboard assays. These assays were repeated twice independently, yielding the same results. **e**, Binding affinity of MAC-545496 and/or its analogs to full-length and truncated G217* GraR as determined by isothermal titration calorimetry. Data are mean ± s.e.m. $n = 5$ (full length with MAC-545496 or analog VI), $n = 4$ (full length with analog I) and $n = 3$ (truncated with MAC-545496). No interaction could be detected for analog VI under the tested conditions. **f**, Dose–response curve of MAC-545496 on the expression of *mprF* following luciferase activity in the wild-type *S. aureus* USA300 background in the presence of 64 μg ml^{-1} colistin at 3 h. $n = 3$ shown as individual replicates in relative light units (RLU), normalized by the culture optical density at 600 nm (OD_{600}); at this n, the power of the assay to detect statistically significant effects at $\alpha = 0.05$ (two tailed) is >99%. Curves are fit by non-linear regression analysis; $r^2 = 0.832$, degrees of freedom = 32. IC_{50} ± s.e.m. = 0.0376 ± 0.027 μg ml^{-1}.

to β-lactams, with no further increase in such susceptibility in the presence of MAC-545496. We screened the NTML at subinhibitory concentrations of cefuroxime (16 and 32 μg ml^{-1}) in the presence and absence of MAC-545496 at 1 and 0.5 μg ml^{-1}, respectively (Fig. 2a,b and Supplementary Fig. 6a). Putative hits comprised mutants in *graR*, *vraF*, *vraG*, SAUSA300_1219 (*desK*) and SAUSA300_1220 (*desR*). Checkerboard assays demonstrated that only the *graR* transposon mutant (*graR*::Tn) clearly showed reduced resistance to cefuroxime (MIC of 4 μg ml^{-1} as compared to 512 μg ml^{-1} for the wild type) and a lack of synergy between the β-lactam and MAC-545496 (Fig. 2c and Supplementary Fig. 6b). Furthermore, the *graR* mutant showed a much higher targocil MIC as compared to the parent strain, phenocopying targocil antagonism with MAC-545496 (Supplementary Fig. 6c). Importantly, Δ*tarO* showed synergy between cefuroxime and MAC-545496, ruling out early step WTA biosynthesis as a target (Supplementary Fig. 6d).

Together, these data suggested that GraR was the target of MAC-545496. Notably, GraR is involved in a synthetic lethal interaction with WTA[15], which may explain the ability of a GraR inhibitor to antagonize the lethal action of targocil and synergize with β-lactams (through the involvement of WTA in spatial and temporal regulation of the major autolysin AtlA and penicillin-binding protein PBP4). The regulatory effects of GraR on AtlA and potentially other components of the GraR regulon[17] might also contribute to the synergy between a GraR inhibitor and β-lactams. Checkerboard analyses of mutants with disruptions in genes encoding the remaining components of the GraXRS VraFG regulatory system and a member of the regulon (MprF) revealed that, with the exception of *graS*::Tn (which behaved similarly to the wild type), these mutants showed partial reduction in resistance to cefuroxime and/or colistin, as well as a partial reduction in synergy of these antibiotics with MAC-545496 as compared to *graR*::Tn (Supplementary Fig. 7). Indeed, signal transduction by phosphotransfer from a stimulated (phosphorylated) GraS to activate GraR by phosphorylating its conserved Asp51 residue may be bypassed by VraFG through GraX[16]. Alternatively, GraR can be phosphorylated and activated by the serine–threonine kinase Stk1, a master regulator of cell-wall homeostasis, substituting at least partially for GraS activities[28]. Together, this may explain the lack of phenotypes in *graS*::Tn as compared to the other mutants. The partial phenotypes of the mutants downstream of GraR in the signal transduction cascade, as well as the lack of it in GraS, together provided further evidence that GraR was the target of MAC-545496. Indeed, the effects of MAC-545496 on the antimicrobial activity of the different classes of antibiotics (Supplementary Fig. 5) matches with reported phenotypes of *graR* disruption in chemical–genomic experiments leading to different degrees of sensitization to CAMPs[29], β-lactam[30], aminoglycosides[29–31], daptomycin[29,30], vancomycin[29,30] and bacitracin[29], with no reported changes in susceptibility to other antibiotics such as D-cycloserine or novobiocin.

Additional confirmation included selection for spontaneous resistant mutants in which MAC-545496 lacked activity. As MAC-545496 is not growth inhibitory against *S. aureus*, this was done in the presence of sub-MIC concentrations of cefuroxime in liquid medium (frequency of resistance $\approx 6.6 \times 10^{-6}$, determined from a separate experiment conducted on solid medium). We tested four of the resulting mutants and they showed no synergism between MAC-545496 and cefuroxime (Fig. 2d and Supplementary Fig. 8a) despite having the same MICs as the wild type for cefuroxime and other antibiotics (vancomycin, tetracycline and gentamicin; Supplementary Fig. 8b), demonstrating the specificity of these mutations to MAC-545496. We sequenced the regions flanking the *graXRS* and *vraFG* operons using Sanger sequencing and mapped the mutation as a G217* nonsense mutation of GraR leading to an 8-amino-acid truncation of its C terminus (G649T single-nucleotide polymorphism in *graR*). Notably, GraR is a member of the OmpR subfamily of response regulators, with a typical winged helix–turn–helix domain extending from residues 173 to 203, whereas its receiver domain extends from residues 1 to 122 with the conserved aspartate residue at 51 (ref. [17]). The two domains are tethered by a flexible linker region as in OmpR family transcriptional factors[32]. Hence, the truncation does not seem to affect the functional domains of the protein, which is consistent with the retention of normal GraR activity in the resistant mutants, which is evident from their β-lactam-resistance phenotype. Furthermore, aligning the full-length GraR to the truncated protein (modeled to either BasR or MtrA, which are other OmpR family proteins) shows that the truncation led to slight conformational changes mostly at the linker region (Supplementary Fig. 8c). Complementation and genetic recapitulation of the MAC-545496-resistance mutation were performed in the *graR*::Tn background; full-length GraR increased resistance to cefuroxime and restored synergy with MAC-545496, whereas the truncated version increased resistance 32-fold but lacked synergy (Supplementary Fig. 9). Next, we determined the binding affinity of MAC-545496 to recombinant GraR protein by isothermal titration calorimetry. MAC-545496 displayed strong binding affinity to the full-length protein ($K_d \leq 0.1$ nM, the quantification limit of the instrument; Fig. 2e and Supplementary Fig. 10). We tested other active and inactive analogs of MAC-545496, analog I (**10**) and analog VI (**15**), respectively (discussed below). These showed high affinity ($K_d \leq 0.1$ nM) and no detectable binding, respectively (Fig. 2e and Supplementary Fig. 10), consistent with the biological activity in whole cells. Furthermore, MAC-545496 bound with almost three orders of magnitude lower affinity to the truncated resistant GraR relative to the full-length protein (Fig. 2e and Supplementary Fig. 10), consistent with the lack of activity of MAC-545496 against the resistant mutants. Notably, circular dichroism confirmed that the secondary structure of the truncated protein was maintained and matched that of full-length GraR; both were in agreement with the predicted secondary structure of the proteins (Supplementary Fig. 11). Together, these data further support the conclusion that GraR is the target of MAC-545496.

Next, we reasoned that inhibition of GraR would attenuate the expression of proteins in its regulon. We followed the expression of *mprF* through a transcriptional fusion with *luxABCDE* using a luciferase expression assay. MAC-545496 inhibited *mprF* expression regardless of colistin induction in the wild-type background (Supplementary Fig. 12a). MAC-545496 showed inhibition of *mprF* expression in a concentration-dependent manner; the half-maximal inhibitory concentration (IC_{50}) was 0.0376 μg ml^{-1}—matching with the concentration range of the synergistic effect with cefuroxime (Fig. 2f). In Δ*graR*, MAC-545496 did not affect *mprF* expression, which was considerably suppressed as compared to the wild-type level (Supplementary Fig. 12b). Notably, in Δ*graS*, MAC-545496 slightly, but significantly, reduced *mprF* expression despite being significantly suppressed relative to the parent strain (Supplementary Fig. 12c). Conversely, we followed the expression of *ilvD* (encoding a protein involved in biosynthesis of branched-chain amino acids[33]) as a negative control; its expression was not affected by colistin or by MAC-545496 (Supplementary Fig. 12d). Together, these findings offer additional support for GraR as the target of MAC-545496.

Effect of MAC-545496 on other bacteria. GraR homologs have been characterized in other Gram-positive bacteria such as *Staphylococcus epidermidis* (GraR, also known as ApsR)[34] and *Listeria monocytogenes* (VirR)[35] showing similar functions as that in *S. aureus*. Coagulase-negative Staphylococci, especially *S. epidermidis*, represent a regular part of the microbiota of the skin and mucous membranes of humans[36]; hence, we tested the activity of MAC-545496 on *S. epidermidis*. Despite the high similarity of the GraXRS VraFG system of *S. epidermidis* to that of *S. aureus*, MAC-545496 did not synergize with cefuroxime against three *S. epidermidis* isolates (Supplementary Fig. 13a), nor did it affect the activity of vancomycin (Supplementary Fig. 13b). Although the GraR homolog of *S. epidermidis* NIH04008 has 91% identity to that of *S. aureus* USA300, aligning the proteins (both modeled to MtrA) shows slight conformational differences mostly at the flexible linker region and the C terminus (Supplementary Fig. 13c) similar to where the full-length *S. aureus* USA300 and truncated GraR were different (Supplementary Figs. 8c and 13c). This might explain the lack of effect of MAC-545496 in *S. epidermidis*. Notably, the GraXRS system is unrelated to the Gram-negative antimicrobial-peptide-sensing systems such as the PhoPQ two-component system. Hence, the lack of activity of MAC-545496 against *Pseudomonas aeruginosa* PAO1, which presented as a lack of synergy with colistin or cefuroxime, was expected (Supplementary Fig. 13d). Together, these findings suggest that MAC-545496 represents a lead with the potential for minimal disruptive effects on the beneficial host flora, one of the features of an ideal antivirulence agent.

MAC-545496 inhibits biofilm formation. *S. aureus* forms biofilms on several medically relevant surfaces such as catheters and intraocular lenses; biofilm formation by this microbe is thought to contribute to its ability to cause persistent infections[37]. Biofilm formation by *S. aureus* is further induced by chelating agents commonly used as anticoagulants in catheter locks and infusions such as citrates[38]; O'Toole and colleagues revealed that the anticoagulant-induced biofilm-formation phenotype depends, in part, on the GraXRS regulatory system[23]. Indeed, MAC-545496 did not show effects on the background biofilm formed by the wild type in the absence of an anticoagulant or biofilms formed by the *graR*::Tn mutant under any of the tested conditions. MAC-545496 only inhibited the citrate-induced biofilm formation in the wild type in a concentration-dependent manner (Fig. 3), suggesting additional potential as a lead for drug discovery.

In cellulo and in vivo efficacy as monotherapy. Intracellular *S. aureus* is considered a reservoir that can systemically disseminate infection even in the presence of antibiotics, potentially leading to clinical failures and relapses after antibiotic therapy[39]. Therefore, complete eradication of intracellular *S. aureus*, especially those inside blood-borne phagocytes, is thought to be key to clinical success. Here we tested the effect of MAC-545496 on *S. aureus* survival in RAW 264.7 macrophages. MAC-545496 at 20 μg ml^{-1} completely inhibited replication of *S. aureus* cells in macrophages detected 12 h after infection whether the cells were pretreated with MAC-545496 before infection or treated after phagocytosis, demonstrating the efficacy of MAC-545496 in cellulo (Supplementary Fig. 14a). Treatment of *S. aureus*-infected macrophages with different doses of MAC-545496 added 30 min after phagocytosis showed that the GraR inhibitor halted *S. aureus* replication within macrophages starting at 0.5 μg ml^{-1} (Fig. 4a). Of note, prolonged incubation with

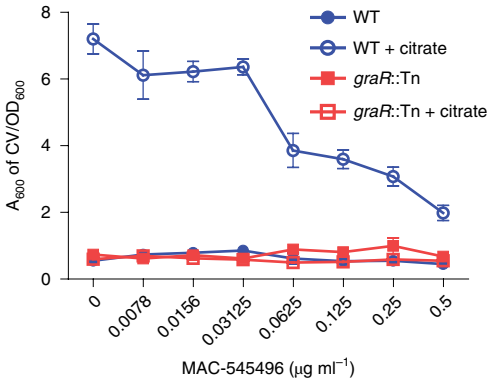

Fig. 3 | MAC-545496 inhibits *S. aureus* USA300 biofilm formation. Crystal violet biofilm assay of *S. aureus* USA300 detected at ~18 h as the absorbance at 600 nm of the solubilized crystal violet that stained the biofilms (A_{600} of CV), normalized by the OD_{600} of the planktonic cells culture. $n = 9$ from three independent experiments (mean ± s.e.m.). The actual power of the assay to detect statistically significant effects at $\alpha = 0.05$ (two tailed) ranged between 95% and 99%.

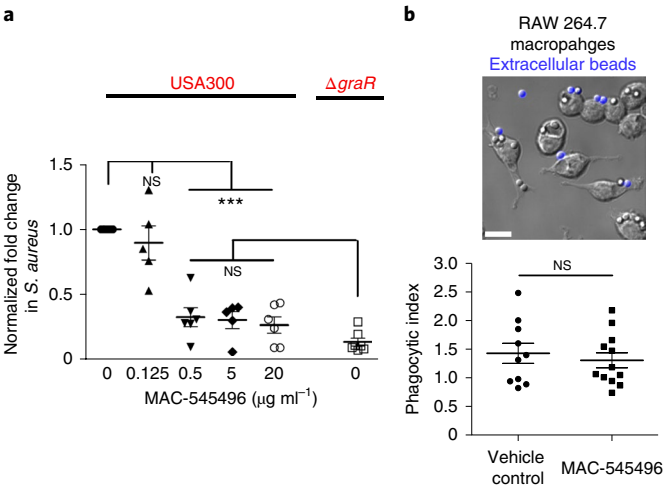

Fig. 4 | MAC-545496 abrogates intracellular survival of *S. aureus* USA300. a, Replication of *S. aureus* in RAW 264.7 macrophages infected with wild type USA300 or Δ*graR* mutant with and/or without MAC-545496 treatment. Data are from three independent experiments, each with two biological replicates, and are shown as the fold change in CFU ml^{-1} (calculated as the CFU ml^{-1} at 12 h divided by the CFU ml^{-1} at 1.5 h, normalized to the corresponding wild-type level with DMSO treatment group). **b**, MAC-545496 does not alter the phagocytic capacity of RAW 264.7 macrophages. Macrophages were treated with 0.5 μg ml^{-1} MAC-545496 for 12 h then exposed to IgG-coated beads for 20 min. The phagocytic index was calculated as the number of internalized beads per cell in each field (mean ± s.e.m). The numbers of fields evaluated (n) were 10 and 12 for control and MAC-545496-treated conditions, respectively (enough to have at least 100 macrophages counted per condition; derived from three independent experiments). A representative micrograph is shown. Scale bar, 10 μm. NS, not significant. ***$P < 0.001$ (two tailed); determined by one-way ANOVA and Bonferroni post hoc correction. The overall P, F and total degrees of freedom were <0.0001, 24.96 and 40, respectively (**a**). At the chosen sample sizes (n), the actual power of the assay to detect statistically significant effects at $\alpha = 0.05$ (two tailed) is >99%.

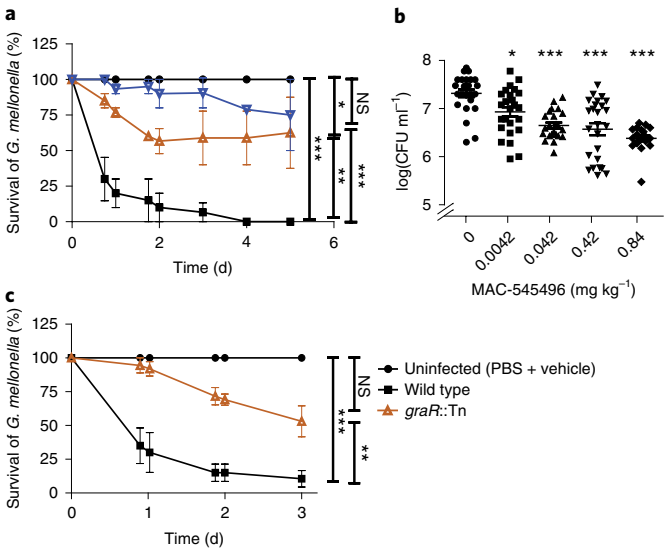

Fig. 5 | MAC-545496 attenuates virulence in vivo. a, The survival of *G. mellonella* larvae infected with *S. aureus* and treated with MAC-545496 at 0.042 mg kg^{-1} (open brown triangles) or 0.42 mg kg^{-1} (open blue inverted triangles) or untreated (solid black squares) as compared to the control group injected with sterile PBS (solid black circles). Ten larvae per group; the results were obtained from three independent experiments and are shown as the mean ± s.e.m. **b**, Numbers of *S. aureus* USA300 (CFU ml^{-1}) recovered from larval hemolymph 200 min after infection. $n = 25$ for all doses (except for 0.042 and 0.84 mg kg^{-1} where $n = 23$ and 19, respectively), from two independent experiments, shown as the mean ± s.e.m. **c**, The survival of *G. mellonella* larvae infected with wild-type *S. aureus* USA300 or the *graR*::Tn mutant as compared to the control group injected with sterile PBS. Ten larvae per group; the results were obtained from four independent experiments and are shown as the mean ± s.e.m. *$P < 0.05$, **$P < 0.01$, ***$P < 0.001$ (two tailed); determined by one-way ANOVA and Bonferroni post hoc correction. The overall P, F and total degrees of freedom were <0.0001, 26.82 and 31 (**a**); <0.0001, 15.62 and 116 (**b**); and 0.0004, 13.99 and 17 (**c**), respectively. At the chosen sample sizes (n), the actual power of the assay to detect statistically significant effects at $\alpha = 0.05$ (two tailed) is >99% (**b**–**e**).

MAC-545496 did not alter the phagocytic index of macrophages—a parameter that would be particularly sensitive to minor toxicities affecting the function of macrophages through a myriad of off-target effects—as compared to the vehicle treatment (Fig. 4b). Recently, Flannagan et al. showed that the GraXRS regulatory system is required to evade killing of *S. aureus* within host antibacterial immune cells including macrophages before commencement of replication therein[21]. Exposure of *S. aureus* to phagolysosome acidification induces the GraXRS system, eliciting an adaptive response that increases resistance to antimicrobial effectors that are encountered inside macrophage phagolysosomes[21]. Treatment with MAC-545496 recapitulated the phenotype of Δ*graR* and Δ*graS* mutants (Fig. 4a and Supplementary Fig. 14a), effectively inhibiting intracellular *S. aureus* growth.

In vivo, MAC-545496 was effective as a monotherapy for MRSA-infected *Galleria mellonella* larvae. Given that MAC-545496 has no effect on viability of *S. aureus* in vitro, we initially performed a concomitant infection with *S. aureus* and treatment with MAC-545496 as a proof of principle by mixing the different doses of the drug into the inoculum suspension immediately before injection into the larvae. MAC-545496 activity was evidenced by increased survival of the drug-treated larvae as compared to infected untreated ones (Fig. 5a). This corresponded to concentration-dependent killing of *S. aureus* in the hemolymph of the larvae observed from the CFUs recovered from the hemolymph 200 min after infection (Fig. 5b). This matched with the attenuated virulence of the *graR*::Tn mutant relative to the wild type in *Galleria* (Fig. 5c). Next, we conducted

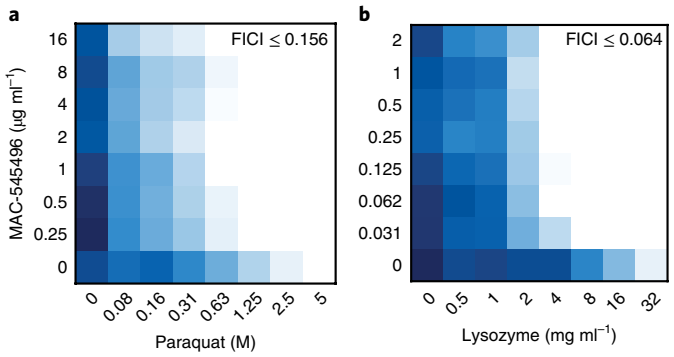

Fig. 6 | MAC-545496 potentiates components of the innate immune response (oxidative stress and lysozyme). a,**b**, Representative checkerboard assays of MAC-545496 with the superoxide-inducing agent paraquat (**a**) and lysozyme (**b**) against *S. aureus* USA300. These assays were repeated three times independently yielding similar results.

other experiments where treatment of *S. aureus*-infected larvae with MAC-545496 occurred 30 min after infection as a more sensitive experimental setup that mimics acquiring bacterial infection before initiating antimicrobial therapy. Larval survival results were similar to those obtained from the concomitant infection–treatment experiments (Supplementary Fig. 15a). They also matched the patterns of CFUs recovered from the hemolymph of the larvae following the different treatments (Supplementary Fig. 15b). Notably, to validate this model of infection we included cefuroxime and vancomycin as negative and positive controls, respectively, as MRSA is resistant and sensitive, respectively, to these drugs. The larval survival and the CFUs recovered from the hemolymph matched with the respective activities of these antibiotics against MRSA (Supplementary Fig. 15). *Galleria* possess an active innate immune response that is mainly driven by cationic antimicrobial peptides in addition to other factors, such as reactive oxygen species and lysozyme. Notably, GraR inhibition by MAC-545496 augmented the potency of the oxidative stress (superoxide)-inducing agent paraquat (Fig. 6a), likely owing to the role of GraR in the response to oxidative stress, which might be attributed to its regulatory activity on MntABC[17], an ATP-binding cassette (ABC)-type transporter for manganese uptake that is involved in the superoxide stress response[40]. In addition, the GraR inhibitor synergized with lysozyme (Fig. 6b). This might be due to the regulatory activity of GraR on several autolysins[17] and/or its genetic interaction with peptidoglycan *O*-acetyltransferase OatA[15], the major determinant for lysozyme resistance[41].

The poor aqueous solubility of MAC-545496 hindered its systemic testing in a mammalian model of infection; however, mutants in the *graXRS* regulatory system have been shown to be severely attenuated in mouse[19,20] and rabbit[42] models of infection, and to be defective in early stage intracellular survival within the mouse liver in vivo[21]. Also, low-virulence isolates from implant-associated bone infections harbored mutations disrupting the GraXRS system, whereas the regulatory system was intact in highly virulent isolates[22]. These reported in vivo phenotypes suggest that GraR inhibition could be efficacious against MRSA infection in animals similar to the effects of MAC-545496 observed in *Galleria*. Notably, the activity of MAC-545496 was not inhibited by human serum owing to binding of plasma protein as it was capable of potentiating cefuroxime activity against *S. aureus* USA300 in the presence of 10% serum (heat-inactivated at 65 °C for 10 min; MAC-545496 at 8 μg ml^{-1} reduced the MIC of cefuroxime from 64 to 8 μg ml^{-1}). Pilot medicinal chemistry efforts were conducted where we synthesized 12 analogs of MAC-545496 providing insights on the structure–activity relationships of MAC-545496 (Supplementary Figs. 16 and 17). The potency was enhanced by increasing the piperidine ring size to an azepane ring, whereas the nitro group could be replaced with other electron-withdrawing groups such as a nitrile group without loss of activity. In addition, while all tested modifications to the chloro-pyridinyl group led to loss of activity, some modifications including the addition of a carboxylic group to this aromatic ring led to a marked increase in aqueous solubility albeit at alkaline pH. These findings will guide future efforts to improve aqueous solubility, while preserving bioactivity. Such an analog would enable further investigation of the promising mechanism of action of MAC-545496 and potentially enable preclinical testing. Together, the synergistic effect of MAC-545496 with components of the innate immune system such as CAMPs, oxidative stress and lysozyme suggest that GraR may represent a viable target for monotherapy.

Discussion

Antivirulence strategies have gained interest in recent years with efforts targeting *S. aureus* virulence factors including staphyloxanthin pigment synthesis, quorum sensing and capsule biosynthesis[43–47]. Also, antibiotic adjuvants represent an emerging strategy to revive already existing antibiotics[48]. GraR, a regulator of the response to cell-envelope stress, has been well characterized over the past decade and has been recognized as an important virulence factor and determinant of antibiotic resistance, making it an ideal target for antimicrobial intervention that was yet to be exploited. Here we discovered an inhibitor against GraR, that can serve a dual role: (i) an antibiotic adjuvant reversing methicillin resistance and allowing dose-sparing of β-lactams and CAMPs; and (ii) an antivirulence agent that could be used as a standalone therapy against MRSA without disrupting the normal flora. Notably, MAC-545496 had no effect on the closely related commensal *S. epidermidis* nor did it affect Gram-negative bacteria such as *P. aeruginosa*. With potency at the low nanomolar range against MRSA, MAC-545496 reverses β-lactam resistance, inhibits biofilm formation, abrogates intracellular survival and attenuates virulence in vivo. Together, this work provides antibacterial leads of a new mechanism expanding our arsenal for combating drug-resistant Staphylococcal infections.

Online content

Any methods, additional references, Nature Research reporting summaries, source data, extended data, supplementary information, acknowledgements, peer review information; details of author contributions and competing interests; and statements of data and code availability are available at https://doi.org/10.1038/s41589-019-0401-8.

Received: 3 December 2018; Accepted: 7 October 2019;
Published online: 25 November 2019

References

1. *Prioritization of Pathogens to Guide Discovery, Research and Development of New Antibiotics for Drug-Resistant Bacterial Infections Including Tuberculosis* (World Health Organization, 2017).
2. Boucher, H. W. et al. Bad bugs, no drugs: no ESKAPE! an update from the Infectious Diseases Society of America. *Clin. Infect. Dis.* **48**, 1–12 (2009).
3. Nannini, E., Murray, B. E. & Arias, C. A. Resistance or decreased susceptibility to glycopeptides, daptomycin, and linezolid in methicillin-resistant *Staphylococcus aureus*. *Curr. Opin. Pharmacol.* **10**, 516–521 (2010).
4. Lowy, F. D. *Staphylococcus aureus* infections. *New Engl. J. Med.* **339**, 520–532 (1998).
5. Wright, G. D. & Sutherland, A. D. New strategies for combating multidrug-resistant bacteria. *Trends Mol. Med.* **13**, 260–267 (2007).
6. Maura, D., Ballok, A. E. & Rahme, L. G. Considerations and caveats in anti-virulence drug development. *Curr. Opin. Microbiol.* **33**, 41–46 (2016).
7. Lee, K., Campbell, J., Swoboda, J. G., Cuny, G. D. & Walker, S. Development of improved inhibitors of wall teichoic acid biosynthesis with potent activity against *Staphylococcus aureus*. *Bioorg. Med. Chem. Lett.* **20**, 1767–1770 (2010).
8. Sewell, E. W. & Brown, E. D. Taking aim at wall teichoic acid synthesis: new biology and new leads for antibiotics. *J. Antibiot.* **67**, 43–51 (2014).

9. D'Elia, M. A., Henderson, J. A., Beveridge, T. J., Heinrichs, D. E. & Brown, E. D. The *N*-acetylmannosamine transferase catalyzes the first committed step of teichoic acid assembly in *Bacillus subtilis* and *Staphylococcus aureus*. *J. Bacteriol.* **191**, 4030–4034 (2009).
10. D'Elia, M. A., Millar, K. E., Beveridge, T. J. & Brown, E. D. Wall teichoic acid polymers are dispensable for cell viability in *Bacillus subtilis*. *J. Bacteriol.* **188**, 8313–8316 (2006).
11. D'Elia, M. A. et al. Lesions in teichoic acid biosynthesis in *Staphylococcus aureus* lead to a lethal gain of function in the otherwise dispensable pathway. *J. Bacteriol.* **188**, 4183–4189 (2006).
12. Lee, S. H. et al. TarO-specific inhibitors of wall teichoic acid biosynthesis restore *β*-lactam efficacy against methicillin-resistant staphylococci. *Sci. Transl. Med.* **8**, 329ra332 (2016).
13. Czarny, T. L. & Brown, E. D. A small-molecule screening platform for the discovery of inhibitors of undecaprenyl diphosphate synthase. *ACS Infect. Dis.* **2**, 489–499 (2016).
14. Farha, M. A. et al. Antagonism screen for inhibitors of bacterial cell wall biogenesis uncovers an inhibitor of undecaprenyl diphosphate synthase. *Proc. Natl Acad. Sci. USA* **112**, 11048–11053 (2015).
15. Santa Maria, J. P. Jr. et al. Compound-gene interaction mapping reveals distinct roles for *Staphylococcus aureus* teichoic acids. *Proc. Natl Acad. Sci. USA* **111**, 12510–12515 (2014).
16. Falord, M., Karimova, G., Hiron, A. & Msadek, T. GraXSR proteins interact with the VraFG ABC transporter to form a five-component system required for cationic antimicrobial peptide sensing and resistance in *Staphylococcus aureus*. *Antimicrob. Agents Chemother.* **56**, 1047–1058 (2012).
17. Falord, M., Mader, U., Hiron, A., Debarbouille, M. & Msadek, T. Investigation of the *Staphylococcus aureus* GraSR regulon reveals novel links to virulence, stress response and cell wall signal transduction pathways. *PLoS One* **6**, e21323 (2011).
18. Yang, S. J. et al. The *Staphylococcus aureus* two-component regulatory system, GraRS, senses and confers resistance to selected cationic antimicrobial peptides. *Infect. Immun.* **80**, 74–81 (2012).
19. Kraus, D. et al. The GraRS regulatory system controls *Staphylococcus aureus* susceptibility to antimicrobial host defenses. *BMC Microbiol.* **8**, 85 (2008).
20. Li, M. et al. The antimicrobial peptide-sensing system *aps* of *Staphylococcus aureus*. *Mol. Microbiol.* **66**, 1136–1147 (2007).
21. Flannagan, R. S., Kuiack, R. C., McGavin, M. J. & Heinrichs, D. E. *Staphylococcus aureus* uses the GraXRS regulatory system to sense and adapt to the acidified phagolysosome in macrophages. *MBio* **9**, e01143-18 (2018).
22. Mannala, G. K. et al. Whole-genome comparison of high and low virulent *Staphylococcus aureus* isolates inducing implant-associated bone infections. *Int J. Med. Microbiol.* **308**, 505–513 (2018).
23. Shanks, R. M. et al. Genetic evidence for an alternative citrate-dependent biofilm formation pathway in *Staphylococcus aureus* that is dependent on fibronectin binding proteins and the GraRS two-component regulatory system. *Infect. Immun.* **76**, 2469–2477 (2008).
24. Campbell, J. et al. An antibiotic that inhibits a late step in wall teichoic acid biosynthesis induces the cell wall stress stimulon in *Staphylococcus aureus*. *Antimicrob. Agents Chemother.* **56**, 1810–1820 (2012).
25. Strauss, L. et al. Origin, evolution, and global transmission of community-acquired *Staphylococcus aureus* ST8. *Proc. Natl Acad. Sci. USA* **114**, E10596–E10604 (2017).
26. *Performance Standards for Antimicrobial Susceptibility Testing* 27th Edition, CLSI Supplement M100 (Clinical and Laboratory Standards Institute, 2017).
27. Fey, P. D. et al. A genetic resource for rapid and comprehensive phenotype screening of nonessential *Staphylococcus aureus* genes. *MBio* **4**, e00537-12 (2013).
28. Fridman, M. et al. Two unique phosphorylation-driven signaling pathways crosstalk in *Staphylococcus aureus* to modulate the cell-wall charge: Stk1/Stp1 meets GraSR. *Biochemistry* **52**, 7975–7986 (2013).
29. Vestergaard, M. et al. Inhibition of the ATP synthase eliminates the intrinsic resistance of *Staphylococcus aureus* towards polymyxins. *MBio* **8**, e01114-17 (2017).
30. Rajagopal, M et al. Multidrug intrinsic resistance factors in *Staphylococcus aureus* identified by profiling fitness within high-diversity transposon libraries. *MBio* **7**, e00950-16 (2016).
31. Vestergaard, M. et al. Genome-wide identification of antimicrobial intrinsic resistance determinants in *Staphylococcus aureus*. *Front. Microbiol.* **7**, 2018 (2016).
32. Martinez-Hackert, E. & Stock, A. M. Structural relationships in the OmpR family of winged-helix transcription factors. *J. Mol. Biol.* **269**, 301–312 (1997).
33. Kaiser, J. C. et al. Repression of branched-chain amino acid synthesis in *Staphylococcus aureus* is mediated by isoleucine via CodY, and by a leucine-rich attenuator peptide. *PLoS Genet.* **14**, e1007159 (2018).
34. Li, M. et al. Gram-positive three-component antimicrobial peptide-sensing system. *Proc. Natl Acad. Sci. USA* **104**, 9469–9474 (2007).
35. Mandin, P. et al. VirR, a response regulator critical for *Listeria monocytogenes* virulence. *Mol. Microbiol* **57**, 1367–1380 (2005).
36. Becker, K., Heilmann, C. & Peters, G. Coagulase-negative staphylococci. *Clin. Microbiol. Rev.* **27**, 870–926 (2014).
37. del Pozo, J. L. & Patel, R. The challenge of treating biofilm-associated bacterial infections. *Clin. Pharm. Ther.* **82**, 204–209 (2007).
38. Shanks, R. M., Sargent, J. L., Martinez, R. M., Graber, M. L. & O'Toole, G. A. Catheter lock solutions influence staphylococcal biofilm formation on abiotic surfaces. *Nephrol. Dial. Transpl.* **21**, 2247–2255 (2006).
39. Lehar, S. M. et al. Novel antibody–antibiotic conjugate eliminates intracellular *S. aureus*. *Nature* **527**, 323–328 (2015).
40. Coady, A. et al. The *Staphylococcus aureus* ABC-type manganese transporter MntABC is critical for reinitiation of bacterial replication following exposure to phagocytic oxidative burst. *PLoS One* **10**, e0138350 (2015).
41. Bera, A., Herbert, S., Jakob, A., Vollmer, W. & Gotz, F. Why are pathogenic staphylococci so lysozyme resistant? The peptidoglycan *O*-acetyltransferase OatA is the major determinant for lysozyme resistance of *Staphylococcus aureus*. *Mol. Microbiol* **55**, 778–787 (2005).
42. Cheung, A. L. et al. Site-specific mutation of the sensor kinase GraS in *Staphylococcus aureus* alters the adaptive response to distinct cationic antimicrobial peptides. *Infect. Immun.* **82**, 5336–5345 (2014).
43. Chen, F. et al. Small-molecule targeting of a diapophytoene desaturase inhibits *S. aureus* virulence. *Nat. Chem. Biol.* **12**, 174–179 (2016).
44. Gao, P., Davies, J. & Kao, R. Y. T. Dehydrosqualene desaturase as a novel target for anti-virulence therapy against *Staphylococcus aureus*. *MBio* **8**, e01224-17 (2017).
45. Nielsen, A. et al. Solonamide B inhibits quorum sensing and reduces *Staphylococcus aureus* mediated killing of human neutrophils. *PLoS One* **9**, e84992 (2014).
46. Wang, L. et al. The therapeutic effect of chlorogenic acid against *Staphylococcus aureus* infection through sortase a inhibition. *Front Microbiol* **6**, 1031 (2015).
47. Li, W. et al. Analysis of the *Staphylococcus aureus* capsule biosynthesis pathway in vitro: characterization of the UDP–GlcNAc C6 dehydratases CapD and CapE and identification of enzyme inhibitors. *Int. J. Med. Microbiol.* **304**, 958–969 (2014).
48. Ejim, L. et al. Combinations of antibiotics and nonantibiotic drugs enhance antimicrobial efficacy. *Nat. Chem. Biol.* **7**, 348–350 (2011).

Methods

Strains and reagents. Supplementary Table 4 lists bacteria and plasmids used in this work. Bacteria were grown in cation-adjusted Mueller Hinton medium (CAMHB) at 37 °C. Antibiotics were obtained from Sigma.

High-throughput screening. The targocil-antagonism screen against *S. aureus* Newman was performed as previously described[14,49]. The secondary screen for cefuroxime synergism against *S. aureus* USA300 followed general screening protocols that have been described previously[50].

Antimicrobial-susceptibility testing. MIC determination and checkerboard assays were conducted following the guidelines of the CLSI for MIC testing by broth microdilution[51]. When accurate MIC values could not be determined, as for MAC-545496, the highest concentration tested was considered to be half the MIC value. Fractional inhibitory concentration indices (FICI) were calculated as $FICI = A/MIC_A + B/MIC_B$, where A and B are the concentrations of two antibiotics required in combination to inhibit bacterial growth and MIC_A and MIC_B are the MIC values for drugs A and B alone. FICI data were interpreted as 'synergy' ($FICI \leq 0.5$), 'antagonism' ($FICI > 4.0$) and 'no interaction or indifference' ($1.0 \leq FICI \leq 4.0$).

Nebraska transposon mutant library screen. Overnight cultures of the NTML (at a 384-well density) were performed using the Singer rotor HDA (Singer Instruments) in CAMHB containing erythromycin (5 μg ml^{-1}). Subsequently, CAMHB with or without cefuroxime and/or MAC-545496 was inoculated using the Singer rotor at a 384-well density. The plates were incubated at 37 °C and optical density at 600 nm (OD_{600}) was read after 24 h.

Selection and characterization of spontaneous resistant mutants. Spontaneous resistant mutants were selected for in liquid culture. In brief, isolated colonies were resuspended in PBS and diluted to a final OD_{600} of 0.05 in 200 μl of CAMHB containing MAC-545496 and cefuroxime set up in 96-well microtiter plates. The drug concentrations were guided by previous checkerboard assays. The following concentrations were used (for MAC-545496 and cefuroxime, respectively): 0.0625 and 16; 0.5 and 64; 1 and 64; 2 and 32; and 2 and 128 μg ml^{-1}. Each combination was tested in triplicate. Plates were incubated at 37 °C for 4 d. Bacteria in wells showing growth were reinoculated by 100-fold dilution into fresh medium containing the same concentrations of the combination and allowed to grow overnight. Potential resistant mutants were streaked out for isolation on CAMHB agar plates. Individual colonies were picked and were passaged three times without selection. Four clones originating from different wells were selected and tested in MIC and checkerboard assays. Genomic DNA was prepared and the region spanning the *graXRS* and *vraFG* operons was PCR amplified and sequenced using Sanger sequencing. Frequency of resistance was determined from a separate experiment conducted on solid medium whereby serial dilutions of an overnight culture of *S. aureus* USA300 were plated on CAMHB + 0.7% agarose control plates and plates containing 2 μg ml^{-1} MAC-545496 and 128 μg ml^{-1} cefuroxime. Plates were incubated at 37 °C for 48 h. Colonies growing in the presence of both drugs were passaged three times without selection and retested in the presence and absence of both drugs to confirm resistance to the combination. This experiment was conducted twice independently yielding similar results and the frequency of resistance was reported as the average of both experiments.

General molecular techniques. Deletion of *graR* was performed using the temperature-sensitive pKOR mutagenesis plasmid and procedure as previously described[52]. In brief, ~1-kb upstream and downstream regions of the target genes were amplified through PCR, digested with SacII and ligated together using T4 DNA ligase. Ligation products were then recombined into the parental pKOR plasmid using Gateway BP Clonase (Thermo Fisher Scientific). The resulting deletion plasmid, pKOR::Δ*graR*, was passaged through *E. coli* DH5α and *S. aureus* RN4220 before electroporation into *S. aureus* USA300. Homologous recombination resulted in in-frame deletion of *graR*, which was confirmed through PCR and DNA sequencing. *S. aureus* USA300 Δ*graR* carrying the pGY*lux*::*mprF* reporter plasmid was constructed by electroporation of pGYlux::*mprF* plasmid previously passaged through *E. coli* DH5α and *S. aureus* RN4220 into *S. aureus* USA300 Δ*graR*. The *E. coli*–*S. aureus* shuttle vector pCN51 was modified to carry *aad9* encoding spectinomycin resistance from pCN55, in place of *ermC*, which encodes erythromycin resistance, to construct pCN51Spc as previously described[53]. *graR* and its C-terminally truncated version were cloned into pCN51Spc; the complementation and control vectors were transformed into the *S. aureus* USA300 *graR*::Tn mutant and wild type following passaging into *E. coli* DC10B as described before[54]. Expression from the cadmium-inducible promoter P_{cad}-*cadC* was induced by 0.1 μM cadmium chloride.

Bioluminescence assays. The luciferase expression assays were conducted as previously described[21] in TSB medium at a final volume of 10 ml in 50-ml falcon tubes.

Protein overexpression and purification. GraR proteins, whether full length or truncated, were overexpressed under previously described conditions[28]. Lysis was achieved using a one-shot cell disrupter (Constant Systems) at 30 kPSI. The resulting supernatant was isolated from the insoluble fraction by centrifugation at 16,100*g* for 60 min at 4 °C. His-tag batch purification was performed using HIS-Select nickel-affinity gel (Sigma-Aldrich). The purified proteins were detected by PageBlue protein-staining solution (Thermo Fisher Scientific) on 12% Mini-PROTEAN TGX Precast Protein Gels (Bio-Rad) and quantified by Nanodrop following dialysis using Slide-A-Lyzer dialysis cassette (Thermo Fisher Scientific).

Isothermal titration calorimetry binding assays. The heat flow resulting from the interactions was measured using a high-sensitivity Nano-ITC low volume instrument (cell effective volume 170 μl; TA Instruments). Before use, solutions were degassed under vacuum to eliminate air bubbles and dissolved gas. MAC-545496 or its analogs were diluted into the protein dialysate buffer and placed in the cell at a concentration of 30 μM and GraR (full length or truncated) was placed in the syringe at a concentration of 135.44 μM. Injections (2 μl) were made every 300 s. Experiments were conducted at 25 °C. Each injection produced a heat of reaction, which was determined by the integration of the heat-flow tracings. The heat of dilution was determined in control experiments by injecting the proteins into the corresponding dialysate buffers and was subtracted from the experimental results. The data analysis and dissociation constant (K_d) determination was conducted for each individual run using the NanoAnalyze data analysis software (v.3.8.0).

Circular dichroism spectroscopy. Circular dichroism spectroscopy was performed with an AVIV circular dichroism model 410 spectrometer. The spectra were recorded from 260 to 195 nm in 0.5-nm intervals in a thermostated quartz cuvette with a path length of 1 mm maintained at 25 °C with an averaging time of 5 s and a 1 nm bandwidth. Circular dichroism spectra were recorded in triplicate and averaged and corrected by subtracting the spectra of the dialysis buffer. Data are reported in millidegrees and converted to mean residue ellipticity (degrees square centimeter per decimole). Wavelength scans were analyzed to determine secondary structure content using the K2D predictive algorithms with DICHROWEB[55].

Biofilm formation assays. Biofilm formation was performed in polystyrene 96-well plates under previously described conditions[23] and detected by the crystal violet method[56].

In vivo infection of *Galleria mellonella* larvae. These assays were performed as previously described[57] with modifications. Isolated colonies of *S. aureus* streaked on CAMHB agar were resuspended in PBS, pH 7.4 and adjusted to an OD_{600} of 0.8 for single injection of concomitant infection and treatment (average CFU recovered from the hemolymph of the larvae at zero time is ~4.4×10^7 CFU ml^{-1}) or an OD_{600} of 0.2 for experiments in which the larvae received two injections to allow spacing between infection and treatment (average CFU recovered from the hemolymph of the larvae at zero time is ~1×10^7 CFU ml^{-1}). MAC-545496 was diluted into the bacterial suspension immediately before injection. The larvae (bred in-house, ~200 mg each) were injected with 10 μl per 100 mg larval weight of the bacterial suspensions or sterile PBS containing the same volume of vehicle, dilution factor of ~1,000-fold (ten larvae per group in each experiment). The larvae were incubated at 30 °C and their viability was checked at regular time intervals. In similar assays, five larvae per group were sacrificed 200 min after infection and the hemolymph was extracted as previously described[57]. This endpoint was chosen to avoid any larval lethality, especially in the group that was infected with *S. aureus* USA300 but not treated with MAC-545496. The hemolymph was immediately serially diluted in PBS and plated on CAMHB agar to quantify the CFU of *S. aureus* recovered from the infected larvae.

Infection of RAW 264.7 macrophages. Wild-type *S. aureus* USA300 and isogenic mutants lacking either *graR* or *graS* genes were streaked onto TSA agar and grown overnight. Isolated colonies of *S. aureus* USA300 were inoculated into 5-ml TSB medium cultures with and without MAC-545496 (2 μg ml^{-1}) and grown overnight at 37 °C with shaking. GraR- and GraS-deficient *S. aureus* were grown similarly but without exposure to the GraR inhibitor.

Stationary-phase cells were washed and diluted in serum-free RPMI (SF-RPMI) and used for infection of RAW macrophages at a multiplicity of infection of ten. One set of replicates for *S. aureus* USA300 contained the GraR inhibitor (20 μg ml^{-1}) so that the drug was present throughout every step of the experiment. Macrophages exposed to bacteria were centrifuged at 277*g* to synchronize infection and after 30 min at 37 °C in 5% CO_2, the medium was replaced with SF-RPMI containing gentamicin (100 μg ml^{-1}) for 1 h. Here, after phagocytosis, another set of *S. aureus* USA300 replicates were exposed to the GraR inhibitor along with gentamicin so that the drug was added after the bacteria were phagocytosed. For wells already treated with MAC-545496, the drug was added too. After gentamicin treatment, one set of wells were lysed by treatment with 0.5 ml of 0.1% Triton X-100 after washing with PBS. The remaining well for each infection was incubated with RPMI containing 5% (vol/vol) non-heat-inactivated FBS until 12 h after infection when the cells were lysed. Lysates were diluted and drop plated onto TSA plates

and CFU was determined. Each experiment had two biological replicates for each condition or strain. The fold change in CFU ml^{-1} was determined for each replicate and was calculated as the CFU ml^{-1} at 12 h divided by the CFU ml^{-1} at 1.5 h. For each replicate the data were normalized to the corresponding wild type with only DMSO treatment. In another set of experiments, titration of MAC-545496 was performed by treating macrophages only after phagocytosis. Toxicity of MAC-545496 (at 0.5 μg ml^{-1}) on RAW macrophages was assessed by determining the phagocytic index using IgG-opsonized beads as previously described[58].

Synthesis of MAC-545496 analogs and their characterization. See Supplementary Methods file (Synthetic procedures).

Statistical analyses. Statistical analyses were conducted with GraphPad Prism 5.0 and details are indicated for each assay in the relevant figure captions. All results are shown as mean ± s.e.m. unless otherwise stated. The sample size was chosen with GraphPad StatMate 2.0 to ensure a minimum of 80% power to detect statistically significant effects at a significance level (α) of 0.05 (two tailed). However, the actual power of most of the assays was >99%. In the case of MIC and checkerboard assays, the experiments were repeated at least three independent times and the experiment showing the most conservative effects (if applicable) was shown and the mean ± s.e.m. of the FICI was reported where applicable.

Reporting Summary. Further information on research design is available in the Nature Research Reporting Summary linked to this article.

Data availability

All data generated or analyzed during this study are included in this published article (and its Supplementary Information files). Source data for Figs. 1–6 are presented with the paper.

References

49. El-Halfawy, O. M. & Brown, E. D. High-throughput screening for inhibitors of wall teichoic acid biosynthesis in *Staphylococcus aureus*. in *Bacterial Polysaccharides: Methods in Molecular Biology* vol. 1954 (ed. Brockhausen, I.) 297–308 (Humana Press, 2019).
50. Zlitni, S., Blanchard, J. E. & Brown, E. D. High-throughput screening of model bacteria. *Methods Mol. Biol.* **486**, 13–27 (2009).
51. *Methods for Dilution Antimicrobial Susceptibility Tests for Bacteria that Grow Aerobically* Approved Standard Ninth Edition CLSI Document M07-A9 (Clinical and Laboratory Standards Institute, 2012).
52. Bae, T. & Schneewind, O. Allelic replacement in *Staphylococcus aureus* with inducible counter-selection. *Plasmid* **55**, 58–63 (2006).
53. Charpentier, E. et al. Novel cassette-based shuttle vector system for gram-positive bacteria. *Appl. Environ. Microbiol.* **70**, 6076–6085 (2004).
54. Grosser, M. R. & Richardson, A. R. Method for preparation and electroporation of *S. aureus* and *S. epidermidis*. *Methods Mol. Biol.* **1373**, 51–57 (2016).
55. Whitmore, L. & Wallace, B. A. DICHROWEB, an online server for protein secondary structure analyses from circular dichroism spectroscopic data. *Nucleic Acids Res.* **32**, W668–W673 (2004).
56. Merritt, J. H., Kadouri, D. E. & O'Toole, G. A. Growing and analyzing static biofilms. *Curr. Protoc. Microbiol.* **Chapter 1**, Unit 1B.1 (2005).
57. Harding, C. R., Schroeder, G. N., Collins, J. W. & Frankel, G. Use of *Galleria mellonella* as a model organism to study *Legionella pneumophila* infection. *J. Vis. Exp.* **81**, e50964 (2013).
58. Flannagan, R. S., Heit, B. & Heinrichs, D. E. Intracellular replication of *Staphylococcus aureus* in mature phagolysosomes in macrophages precedes host cell death, and bacterial escape and dissemination. *Cell Microbiol.* **18**, 514–535 (2016).

Acknowledgements

We thank A. Keddie from the University of Alberta for providing valuable advice on breeding *Galleria* and supplying the first batch of larvae, and B. Weber and A. Khaled for their help in breeding *Galleria*. We thank G. Wright from McMaster University for providing *S. aureus* clinical isolates. We also thank S. French for preparing the graphical abstract. This work was supported by grants from the Canadian Institutes of Health Research (foundation grant FRN-143215), the Canadian glycomics network (GlycoNet, https://doi.org/10.13039/501100009056, a National Centre of Excellence) and a Tier I Canada Research Chair award to E.D.B. D.E.H. acknowledges operating grant support from Cystic Fibrosis Canada. Studies performed in the laboratory of M.G.O. were funded by the Ontario Research Foundation. O.M.E.-H. was supported by a Michael G. DeGroote Fellowship Award in Basic Biomedical Science.

Author contributions

O.M.E.-H., T.L.C. and E.D.B. conceived and designed the research. O.M.E.-H. performed all experiments and analyzed all data unless otherwise stated. T.L.C. performed the primary screen. R.S.F. performed the macrophage intracellular assays, supervised by D.E.H. R.C.K. constructed promoter–reporter transcriptional fusions, supervised by M.J.M. J.D., A.S. and P.E. synthesized and characterized MAC-545496 analogs, supervised by M.G.O. J.C.B. helped O.M.E.-H. perform and analyze the ITC assays and performed the circular dichroism assays, supervised by R.M.E. O.M.E.-H and E.D.B. wrote the paper. All authors approved the final version.

Competing interests

E.D.B., O.M.E.-H., T.L.C., J.D., M.G.O., R.S.F. and D.E.H. are inventors on a patent application on the use of MAC-545496 and analogs thereof, alone and in combination with other antibiotics, for the treatment of MRSA infections.

Additional information

Supplementary information is available for this paper at https://doi.org/10.1038/s41589-019-0401-8.

Correspondence and requests for materials should be addressed to E.D.B.

Reprints and permissions information is available at www.nature.com/reprints.

nature research

Corresponding author(s): Eric D. Brown

Last updated by author(s): Sep 14, 2019

Reporting Summary

Nature Research wishes to improve the reproducibility of the work that we publish. This form provides structure for consistency and transparency in reporting. For further information on Nature Research policies, see Authors & Referees and the Editorial Policy Checklist.

Statistics

For all statistical analyses, confirm that the following items are present in the figure legend, table legend, main text, or Methods section.

n/a	Confirmed	
☐	☒	The exact sample size (*n*) for each experimental group/condition, given as a discrete number and unit of measurement
☐	☒	A statement on whether measurements were taken from distinct samples or whether the same sample was measured repeatedly
☐	☒	The statistical test(s) used AND whether they are one- or two-sided *Only common tests should be described solely by name; describe more complex techniques in the Methods section.*
☐	☒	A description of all covariates tested
☐	☒	A description of any assumptions or corrections, such as tests of normality and adjustment for multiple comparisons
☐	☒	A full description of the statistical parameters including central tendency (e.g. means) or other basic estimates (e.g. regression coefficient) AND variation (e.g. standard deviation) or associated estimates of uncertainty (e.g. confidence intervals)
☐	☒	For null hypothesis testing, the test statistic (e.g. *F*, *t*, *r*) with confidence intervals, effect sizes, degrees of freedom and *P* value noted *Give P values as exact values whenever suitable.*
☒	☐	For Bayesian analysis, information on the choice of priors and Markov chain Monte Carlo settings
☒	☐	For hierarchical and complex designs, identification of the appropriate level for tests and full reporting of outcomes
☐	☒	Estimates of effect sizes (e.g. Cohen's *d*, Pearson's *r*), indicating how they were calculated

Our web collection on statistics for biologists contains articles on many of the points above.

Software and code

Policy information about availability of computer code

Data collection	Commercial and publicly available softwares were used and are stated in the manuscript.
Data analysis	Commercial and publicly available softwares were used and are stated in the manuscript: GraphPad Prism 5.0 and GraphPad StatMate 2.0

For manuscripts utilizing custom algorithms or software that are central to the research but not yet described in published literature, software must be made available to editors/reviewers. We strongly encourage code deposition in a community repository (e.g. GitHub). See the Nature Research guidelines for submitting code & software for further information.

Data

Policy information about availability of data

All manuscripts must include a data availability statement. This statement should provide the following information, where applicable:

- Accession codes, unique identifiers, or web links for publicly available datasets
- A list of figures that have associated raw data
- A description of any restrictions on data availability

All data generated or analysed during this study are included in this published article (and its supplementary information files).

Field-specific reporting

Please select the one below that is the best fit for your research. If you are not sure, read the appropriate sections before making your selection.

☒ Life sciences ☐ Behavioural & social sciences ☐ Ecological, evolutionary & environmental sciences

Life sciences study design

All studies must disclose on these points even when the disclosure is negative.

Sample size	The sample size was chosen with GraphPad StatMate 2.0 to ensure a minimum of 80% power to detect statistically significant effects at a significance level (alpha) of 0.05, two tailed. However, the actual power of most of the assays was > 99%. In the case of MIC and checkerboard assays, the experiments were repeated at least three independent times and the experiment showing the most conservative effects (if applicable) was shown and the mean ±S.E.M. of the FICI was reported where applicable.
Data exclusions	No data were excluded from the analyses.
Replication	High throughput primary and secondary screens were performed in duplicate with a very high degree of replication. Bioactives from the screens were further tested and re-supplied and their activity was re-confirmed. Otherwise, all experiments included technical and biological repeats to confirm the replication of the reported effects. All of the reported results were reproducible.
Randomization	Randomization is not relevant to this study since the same bacterial or cell culture is aliquoted and each aliquot received a different treatment with all the appropriate controls running side-by-side. Also, all Galleria larvae were bred in-house to similar weight/size and those deemed equivalent were used in the assays.
Blinding	Blinding is not relevant to this study because all measurements are not subject to investigator's bias or ambiguity since they were either machine collected (for example, absorbance and luminescence reading) or by counting discrete colonies or live/dead larvae.

Reporting for specific materials, systems and methods

We require information from authors about some types of materials, experimental systems and methods used in many studies. Here, indicate whether each material, system or method listed is relevant to your study. If you are not sure if a list item applies to your research, read the appropriate section before selecting a response.

Materials & experimental systems

n/a	Involved in the study
☐	☒ Antibodies
☐	☒ Eukaryotic cell lines
☒	☐ Palaeontology
☐	☒ Animals and other organisms
☒	☐ Human research participants
☒	☐ Clinical data

Methods

n/a	Involved in the study
☒	☐ ChIP-seq
☒	☐ Flow cytometry
☒	☐ MRI-based neuroimaging

Antibodies

Antibodies used	IgG from human serum, Millipore Sigma, cat# I4506 Goat-anti human IgG-AlexaFluor-647, Jackson ImmunoResearch, Cat# 109-605-003 Silica beads, BANGS laboratories Inc., Cat# SS05001
Validation	IgG from human serum, Millipore Sigma, cat# I4506, made latex beads efficient phagocytic targets that were ingested by RAW cells Goat-anti human IgG-AlexaFluor-647, Jackson ImmunoResearch, Cat# 109-605-003, selective reactivity after 2 minute incubation with latex beads only when opsonized with human IgG.

Eukaryotic cell lines

Policy information about cell lines

Cell line source(s)	RAW 264.7 cells were purchased directly from the ATCC.
Authentication	Purchased cells come with a certificate of analysis from ATCC. Additional authentication was not performed. RAW 264.7 (ATCC TIB-71TM), lot# 70000171 and verified by cytochrome C oxidase I (COI) assay by the ATCC.
Mycoplasma contamination	Mycoplasma testing was not formally performed however periodic DAPI staining was done and cultures were free of aberrant or additional DAPI signal other than the host cell nucleus.
Commonly misidentified lines (See ICLAC register)	None. We only used RAW 264.7 from the ATCC.

Animals and other organisms

Policy information about studies involving animals; ARRIVE guidelines recommended for reporting animal research

Laboratory animals	The study did not involve laboratory animals.
Wild animals	The study did not involve wild animals.
Field-collected samples	The study did not involve samples collected from the field.
Ethics oversight	No ethical approval or guidance was required. The study included the use of the Greater wax moth (Galleria mellonella) larvae and bacteria. Both of which do not require ethics approval.

Note that full information on the approval of the study protocol must also be provided in the manuscript.